Predicting vertical LNAPL distribution in the subsurface under the fluctuating water table effect

Lamine Boumaiza[1,2], Romain Chesnaux[1,2], Julien Walter[1,2], Robert J. Lenhard[3], Seyed Majid Hassanizadeh[4,5], Zoi Dokou[6], Motasem Y. D. Alazaiza[7]

[1] Département des Sciences appliquées, Université du Québec à Chicoutimi, Saguenay, Québec, G7H 2B1, Canada

[2] Centre d'études sur les ressources minérales, Groupe de recherche Risque Ressource Eau, Université du Québec à Chicoutimi, Saguenay, Québec, G7H 2B1, Canada

[3] Independent research scientist, San Antonio, TX 78253, USA

[4] Stuttgart Center for Simulation Science (SIMTECH), Integrated Research Training Group SFB 1313, Stuttgart University, Stuttgart, 70049, Germany

[5] Department of Earth Sciences, Environmental Hydrogeology Group, Utrecht University, Utrecht, 3584 CB, The Netherlands

[6] Department of Civil Engineering, California State University, Sacramento, CA 95819, USA

[7] Department of Civil and Environmental Engineering, College of Engineering, A'Sharqiyah University, Ibra, 400, Oman

Corresponding author: E-mail address: lamine.boumaiza@uqac.ca (L. Boumaiza)

This article has been accepted for publication and undergone full peer review but has not been through the copyediting, typesetting, pagination and proofreading process which may lead to differences between this version and the Version of Record. Please cite this article as doi: 10.1111/gwmr.12497

Abstract

The present study proposes a methodology for predicting the vertical LNAPL distribution within an aquifer by considering the influence of water table fluctuations. The LNAPL distribution is predicted by combining (i) information on air/LNAPL and LNAPL/water interface elevations with (ii) the initial elevation of the water table without LNAPL effect. Data used in the present study were collected during groundwater monitoring undertaken over a period of four months at a LNAPL-impacted observation well. In this study, the water table fluctuations raised the free LNAPL in the subsurface to an elevation of 206.63 m, while the lowest elevation was 205.70 m, forming a thickness of 0.93 m of LNAPL-impacted soil. Results show that the apparent LNAPL thickness in the observation well is found to be 3 times greater than the actual free LNAPL thickness in soil; a finding that agrees with previous studies reporting that apparent LNAPL thickness in observation wells typically exceeds the free LNAPL thickness within soil by a factor estimated to range between 2 and 10. The present study provides insights concerning the transient variation of LNAPL distribution within the subsurface and highlights the capability of the proposed methodology to mathematically predict the actual LNAPL thickness in the subsurface, without the need to conduct laborious field tests. Practitioners can use the proposed methodology to determine by how much the water table should be lowered, through pumping, to isolate the LNAPL-impacted soil within the unsaturated zone, which can then be subjected to in-situ vadose zone remedial treatment.

Keywords:

Groundwater monitoring, observation well, impacted soil, apparent LNAPL thickness, free LNAPL, residual LNAPL.

List of variables and abbreviations

CD_{WT}: Corrected depth of the water table
$D_{LNAPL/PVC}$: LNAPL depth relative to the top of the observation well's PVC pipe
GLF: General Levelling of France
h_d^{AN}: Air/LNAPL displacement height
h_d^{NW}: LNAPL/Water displacement height
h_d^{AW}: Air/Water displacement height
h_N: Thickness of free LNAPL in soil
H_N: Apparent LNAPL thickness in observation well
h_{Nt}: Total LNAPL thickness in soil
LNAPL: Light Non-Aqueous Phase Liquid
p_d^{AN}: Air/LNAPL displacement pressure
p_d^{AW}: Air/Water displacement pressure
p_d^{NW}: LNAPL/Water displacement pressure
SD_{WT}: Measured static depth of groundwater
Z_{AN}: Top elevation of free LNAPL in observation well
Z_{AW}: Initial elevation of the water table without LNAPL effect
$ZB\ h_{Nt}$: Bottom elevation of LNAPL-impacted soil
Z_{PVC}: Elevation of the top of the PVC's observation well
$ZT\ h_{Nt}$: Top elevation of LNAPL-impacted soil
ρ_W: Density of water
ρ_N: Density of LNAPL
ρ_A: Density of air
g: Gravitational acceleration
θ: Contact angle
σ_{NW}: Interfacial tension of LNAPL/Water system
σ_{AW}: Interfacial tension of Air/Water system

1 Introduction

Soil and groundwater contamination by petroleum hydrocarbon liquids is a common problem worldwide due to spills during transportation, as well as storage tank and pipeline leakage (Adegboye et al., 2019; Millette et al., 2014). Among petroleum hydrocarbon liquids, those that are lighter than water—known as Light Non-Aqueous Phase Liquids (LNAPL)—typically behave as a separate immiscible phase in the subsurface. LNAPLs have been the subject of many research studies because they pose serious risks to human health and the environment due to their perceived toxicity and longevity. Moreover, LNAPL-impacted site management and remediation activities are challenging due to their complex nature (Charbeneau et al., 2000; Ebrahimi et al., 2019; EPA, 1996; Tomlinson et al., 2017). When LNAPL is released into the subsurface, it migrates downward through the unsaturated zone under gravity and, if sufficient quantities are present, it may reach the saturated zone where it spreads laterally, forming a LNAPL lens (Jeong and Charbeneau, 2014). If the LNAPL is present in sufficient quantity, it can also displace water from some pores below the water table. The earlier LNAPL conceptual models assumed that all the LNAPL is mobile within the soil (e.g., Farr et al., 1990; Lenhard and Parker, 1990). Since then, based on laboratory experiments and field observations, it has been understood that LNAPL can exist in the subsurface under varying forms (Azimi et al., 2020; Frollini and Petitta, 2018; Lenhard et al., 1993; Marinelli and Durnford, 1996). Some of the LNAPL may be at a high saturation, allowing it to flow easily within the connected pores of the soil when subjected to hydraulic gradients. Under this condition, the mobile LNAPL is commonly referred to as free LNAPL. However, other LNAPL present in soil can be immobile, or only negligibly mobile, under certain conditions, including: (i) following the transport of free LNAPL from the ground surface to the water table, where it can be trapped within the flowing pathways; (ii) after the

pumping recovery of the free LNAPL from the impacted aquifer; and (iii) above and below free LNAPL due to water table fluctuations (Charbeneau et al., 2000, 1999; Lefebvre, 2010). In this third situation, some of the free LNAPL may be present as discontinuous ganglia within the aquifer saturated zone. Another LNAPL portion may be entrapped in the form of residual saturation (immobile) within the soil pores—both in the unsaturated and saturated zones—this is referred to as residual LNAPL. This entrapment phenomenon decreases the free LNAPL volume within the aquifer while concurrently increasing the residual LNAPL volume (Chompusri et al., 2002; Lenhard et al., 1993, 2018; Pasha et al., 2014; Sookhak Lari et al., 2018; Steffy et al., 1995; White et al., 2004). Common practices for environmental characterization of LNAPL-impacted sites usually involve drilling boreholes and installing observation wells. Based on the LNAPL thickness measured in observation wells (commonly, and hereinafter in this study, referred to as ‘‘apparent LNAPL thickness’’), the approximate volume of recoverable LNAPL is usually predicted (Jeong and Charbeneau, 2014; Lenhard et al., 2017). In-situ remediation is often preceded by an attempt to hydraulically remove free LNAPL out of an aquifer. The most common in-situ LNAPL remediation approaches include soil vapor extraction, bioventing, thermal methods, enhanced bioremediation and multiphase extraction; often, two to three of these remediation approaches are combined during the remediation activities (Khan et al., 2004; Sookhak Lari et al., 2018, 2020). While the multiphase extraction (application of a vacuum along with LNAPL and water extraction) recovers free LNAPL, impacted groundwater, and soil gas to enhance LNAPL-impacted-mass removal across all phases (Sookhak Lari et al., 2018, 2020; Suthersan et al., 2017), the effectiveness and feasibility of the other remediation approaches may be limited by the groundwater fluctuation effect. Groundwater fluctuations increase the distribution and volume of immobile LNAPL (Lenhard et al., 2018; Pasha et al., 2014) which, if

not removed, may remain as an ongoing source of contamination in an aquifer. When it is submerged within the aquifer saturated zone, immobile LNAPL is not easily removed by means of active remediation approaches (Lekmine et al., 2017; Lenhard et al., 2018; Sookhak Lari et al., 2019). The current literature does not provide extensive detail regarding how to execute an effective in-situ LNAPL remedial plan using optimal in-situ treatments; therefore, the feasibility of an in-situ remediation approach is a question to be answered prior to any remedial project. Alternative solutions addressing (1) how to predict the free and residual LNAPL vertical distribution in the subsurface relative to transient LNAPL/water table fluctuations effect, and (2) how to accurately determine to what extent the water table should be lowered, by means of pumping, in order to isolate the LNAPL in an unsaturated zone and to apply an in-situ unsaturated-zone remediation treatment, have not been jointly addressed in any comprehensive study. The objective of the present study consists, accordingly, in developing a novel predictive approach responding to these two above points; first we introduce the main challenges related to a such development leading to an effective remedial plan.

Observation wells are typically used to monitor the free LNAPL and groundwater fluctuations within the aquifers. Early investigators assumed that there is a direct and relatively simple relationship between the apparent LNAPL thickness in the observation well and the LNAPL thickness within the soil (Lenhard et al., 2017; Van Dam, 1967) (commonly, and hereinafter in this study, the LNAPL thickness within the soil is referred to as the ‘‘actual LNAPL thickness’’). In reality, however, the relationship between the apparent LNAPL thickness in the observation well and the actual LNAPL thickness in the soil is complex (Ballestero et al., 1994; Deska and Ociepa, 2013; EPA, 1996; Farr et al., 1990; Gatsios et al., 2018; Lenhard and Parker, 1990). Due to the potential delay between the LNAPL movement in the soil and that in the

observation well, the thickness of the apparent LNAPL in the observation well can vary significantly—and may even disappear from the observation well during the entire period of elevated water table levels—underpinning a complex relationship between the actual LNAPL thickness in a soil and the apparent LNAPL thickness in an observation well (Aral and Liao, 2002; Atteia et al., 2019; Steffy et al., 1998). Some methods have been proposed for evaluating the actual LNAPL thickness in soil based on the Bail-Down test, which consists of rapid removal of as much of the LNAPL in an observation well as is practical, followed by monitoring of the elevations of the LNAPL/air and LNAPL/water interfaces in the observation well (Gruszcenski, 1987; Hughes et al., 1988; Wagner et al., 1989; Yaniga and Demko, 1983). However, this type of in-situ test is laborious as it requires considerable time and effort to pump and measure the LNAPL, as well as managing the free LNAPL and impacted groundwater pumped during the test. Furthermore, the accurate interpretation of the Bail-Down test data that is used to assess the actual LNAPL thickness is still under discussion (Ahmed et al., 2019; Batu, 2012; Dippenaar et al., 2005; Jeong and Charbeneau, 2014; Palmier et al., 2017). On the other hand, some analytical models have been proposed for predicting the LNAPL distribution in the subsurface. Parker et al. (1994) were among the first who considered the entrapped and residual LNAPL in the soil. However, they did not determine elevation-dependent entrapped or residual LNAPL saturations. Later, Lefebvre and Boutin (2000) presented a LNAPL distribution model based on the Brooks and Corey (1964) soil capillary pressure concept. Their model considers the relationship between fluid distribution (air, water and LNAPL saturations) in the soil adjacent to a LNAPL-impacted observation well. Later, Charbeneau (2007) proposed the LNAPL distribution and recovery model which assumes that vertical equilibrium conditions apply so that the LNAPL distribution can be predicted directly from the elevations of the air/LNAPL interface and the LNAPL/water

interface, measured in an observation well. The considerable gain from those research efforts was the use of the capillary-pressure-saturation relations to predict LNAPL distribution in the soil, by incorporating the elevation of the air/LNAPL interface and of the LNAPL/water interface in the observation well. This makes it possible to determine the influence of the water table fluctuations by monitoring the evolution of LNAPL thickness relative to the water table fluctuations. In relatively recent efforts, researchers have used linear and nonlinear optimization models coupled with numerical models to develop effective remediation strategies consistent with complex objective functions (Atteia et al., 2019; Dokou and Karatzas, 2013; Matos de Souza et al., 2016; Qin et al., 2009; Sookhak Lari et al., 2019). For such numerical models, multiple variables including LNAPL and subsurface properties, as well as initial and boundary conditions, need to be known (e.g., the rate and volume of LNAPL released into the subsurface, the timing and magnitude of potential fluid saturation path changes from precipitation and water table fluctuations, etc.), but these data require more effort to implement and are usually very uncertain (Lenhard et al., 2017). Furthermore, such numerical models are often constrained by ineffective data resulting from unsuitable well locations and inconsistent time trends over the monitoring period (Mobile et al., 2016). Also, multiphase flow and transport codes may be less practical because they are computationally intensive and typically require sophisticated facilities with high associated costs related to training to use the models (Ebrahimi et al., 2019; Lenhard et al., 2017; Parker et al., 2010). It was in this context and considering the above limitations that a simplified methodology—requiring minimum input variables and easy to implement—for predicting the vertical LNAPL distribution in the subsurface appeared to be an attractive alternative solution contributing to more effective remedial plans. A methodology is proposed in this study that contribute to the existing body of literature by (i) mathematically predicting the actual LNAPL

thickness in the subsurface without the need for laborious field tests requiring time-consuming technical LNAPL pumping/monitoring; and (ii) providing insights concerning the transient variations of the LNAPL in the subsurface as a function of the transient variations in elevations of the air/LNAPL and LNAPL/water interfaces in an observation well. Practitioners can use the proposed methodology, which is easy to implement, in their remediation efforts to assess the vertical LNAPL distribution more accurately in a subsurface by considering the transient water table fluctuations effect. The present study provides a methodology for predicting the vertical LNAPL distribution in the subsurface under the fluctuating water table effect, but it is not oriented towards evaluating the recoverable LNAPL volume from the subsurface. In particular, the proposed methodology is capable of determining the depth at which the water table should be lowered by pumping in order to isolate the LNAPL in an unsaturated zone, so that it can then be subjected to in-situ unsaturated-zone remediation treatments (e.g., soil vapor extraction, bioventing). The methodology proposed in the present study is instrumented via periodic measurements of the water table level and apparent LNAPL thickness at a LNAPL-impacted observation well. The methodology is instrumented by data from a single LNAPL-impacted observation well; and it is assumed that the monitored well has been impacted by the lateral transport of LNAPL from a distant LNAPL source, but the lateral extent of LNAPL around the impacted observation well is not addressed in the present study.

2 Collected data and observed LNAPL behavior

An accidental spill of petroleum hydrocarbon liquids occurred at a site located in the Grenoble region of France in 2013. At the impacted site, the water table elevations and apparent LNAPL thickness were monitored in an existing observation well over a period of four months, wherein 15 measurement events were conducted between November 11, 2013, and February 27, 2014.

Subsequent to this accidental spill, additional observation wells were installed at the impacted site as part of an environmental characterization study being carried out prior to in-situ treatment of contaminated soil. The monitored observation well (Figure 1) has a diameter of 51 mm and was completed to a depth of 5.2 m below ground surface. According to the information obtained, the screened section of the observation well has never been completely submerged in the groundwater. Even at the highest water table-level event, the LNAPL have always remained below the top of the screened section of the monitored well, thus allowing the free LNAPL to move inside the observation well at all elevations. The latter was completed with a flush-mount casing, with the top of the PVC riser measured 2 cm below the ground surface. The aquifer geology at the monitoring well consists of natural native sand overlaid by 1.5 m of heterogeneous backfill, composed mainly of a layer of sand with pebbles and sometimes a little clay (Figure 1).

Figure 2 shows the water table depth and the apparent LNAPL thickness within the observation well throughout the monitored period (November 11, 2013 to February 27, 2014). The water table depth ranged from 3.23 to 3.69 m below the ground surface, whereas the measured apparent LNAPL thickness ranged between 0.28 and 0.69 m. The apparent LNAPL fluctuations (change in LNAPL thickness) recorded within the monitored well indicate that apparent LNAPL thicknesses were likely influenced by the water table fluctuations. From the measurement event 1 (November 11, 2013) to the subsequent measurement event 2 (November 27, 2013), the water table depth increases from 3.3 to 3.58 m GLF, while the apparent LNAPL thickness decreases from 0.41 to 0.37 m, denoting an inverse correlation between the water table depth and the apparent LNAPL thickness. This inverse correlation is also observed between the measurement events 9–10 and the measurement events 10–11. However, the predominant relationship observed between the water table depth and the apparent LNAPL thickness, across

11 observations, shows a positive correlation. This means that when the water table depth decreases (i.e., the water table level rises relative to ground surface), the apparent LNAPL thickness decreases in the observation well, and vice versa. As an example, between the measurement event 14 (February 10, 2014) and the subsequent measurement event 15 (February 27, 2014), the water table depth decreases from 3.26 to 3.21 m GLF and the apparent LNAPL thickness also decreases from 0.69 to 0.62 m. This predominantly positive correlation observed between the water table depth and the apparent LNAPL thickness is characteristic of unconfined hydrogeologic conditions (Deska and Ociepa, 2013).

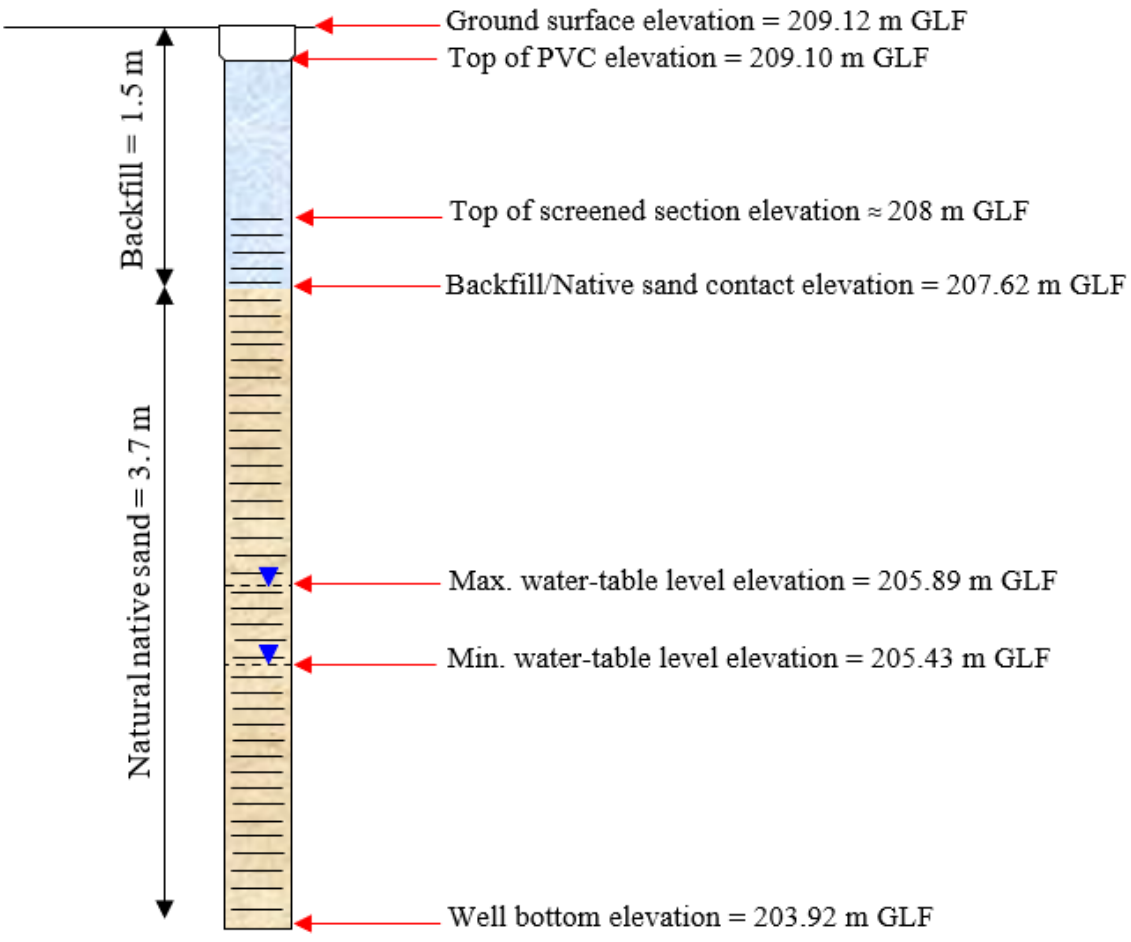

Figure 1. Configuration of the monitored well showing elevations relative to the General Levelling of France (GLF).

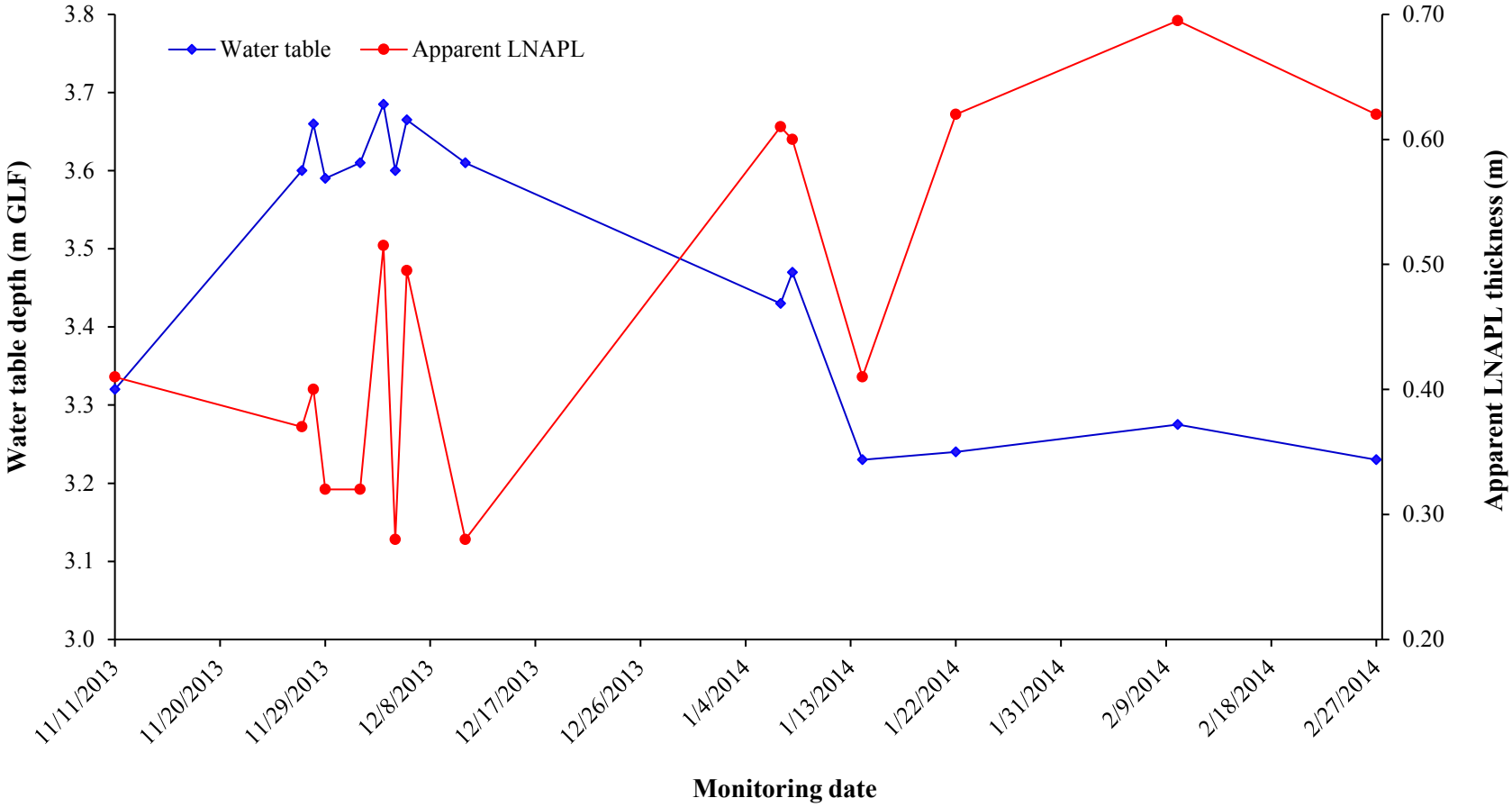

Figure 2. Variations in the monitored well of: (i) water table depth below ground surface, and (ii) apparent LNAPL thickness. The 15 measurement events were conducted at irregular intervals during the monitoring period, as can be observed in Table 1. Nonetheless, the dates on the x-axis of Figure 2 are presented according to a simplified regular interval of 9 days starting from November 11, 2013, to February 27, 2014.

3 Description of the proposed methodology

Figure 3 summarizes the methodology proposed in the present study. It considers the water table level and apparent LNAPL thickness periodically measured in the monitored well over a period of four months. The elevations of the air/LNAPL and LNAPL/water interfaces in the subsurface are mathematically deduced from Lefebvre and Boutin's model (Lefebvre and Boutin, 2000) presented in Figure 4. This model shows the theoretical equilibrium distributions of air, LNAPL and water in the soil and in the screened casing (equivalent to an observation well) based on the capillary pressure model of Brooks and Corey (1964). In Figure 4, to simplify, fluid heights have been used instead of capillary pressures, which are also consistent for determining the displacement heights of the air/LNAPL, LNAPL/water and air/water systems. The total vertical thickness of LNAPL-impacted soil (h_{Nt}) (Figure 4) is estimated by Equation 1 summing the thickness of free LNAPL in soil (h_N) and the air/LNAPL displacement height (h_d^{AN}) (Steps 1 and 2 in Figure 3). h_N is defined as the difference in elevations between the location where the air/LNAPL capillary pressure is zero (Z_{AN} in Figure 4) and where LNAPL will enter a water-saturated soil (p_d^{NW} in Figure 4). LNAPL in this zone will be under positive pressure and will be mobile. The h_d^{AN} indicates where air enters a LNAPL-saturated soil and displaces LNAPL from soil pores; this will occur when the air-LNAPL capillary pressure head reaches the value of h_d^{AN}. For the air-LNAPL-water system, in which LNAPL has intermediate wettability between water and air, h_d^{AN} corresponds to p_d^{AN} in Figure 4. h_d^{AN} is measured from the elevation where the air/LNAPL capillary pressure is zero as underlined by Z_{AN} in Figure 4 (i.e., fully liquid saturated). Methods to calculate h_N and h_d^{AN} are described in the following subsections.

$$h_{Nt} = h_N + h_d^{AN} \quad (1)$$

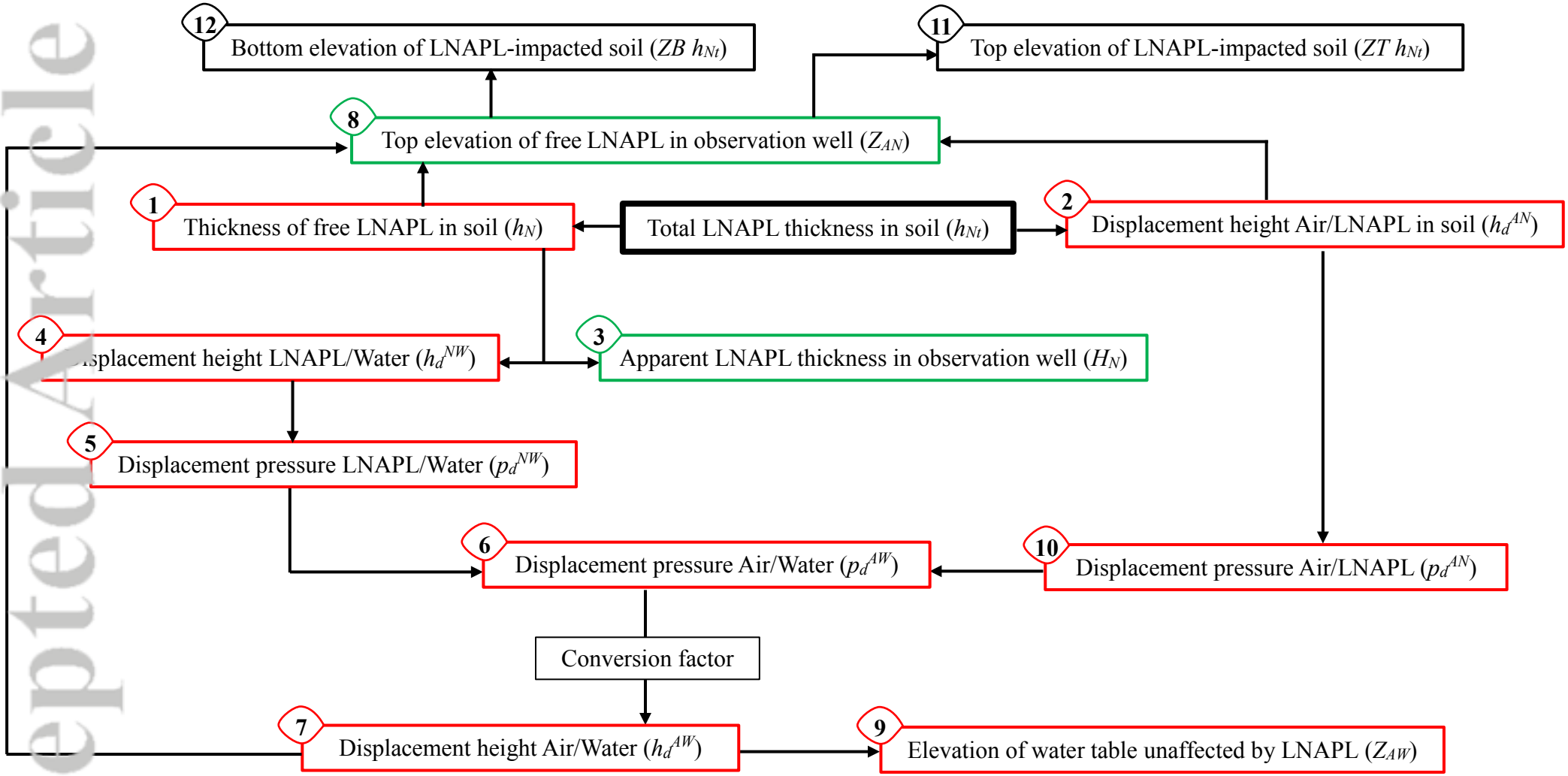

Figure 3. Flowchart for predicting LNAPL-impacted soil thickness and its vertical distribution within an aquifer. The numbers indicate the steps to follow sequentially from 1 to 12; descriptions are detailed in the text. To follow the flowchart steps, the green rectangles include available information data collected from fieldwork, while the black rectangles indicate the value required to obtain the objective. The red rectangles include the parameters to be calculated for which mathematical equations are used. These equations are detailed in the text.

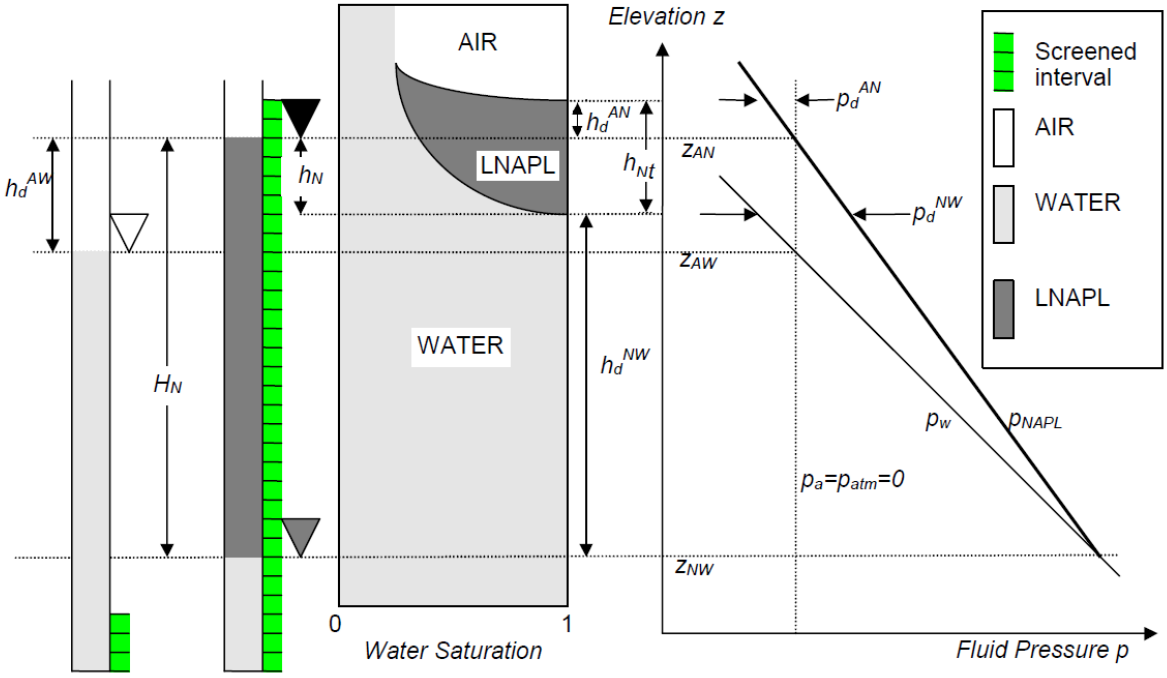

Figure 4. Theoretical representation of the equilibrium of fluid distribution in soil adjacent to a well containing free LNAPL (Adapted from Lefebvre and Boutin, 2000). This model considers the theoretical distributions of air, LNAPL and water in the soil adjacent to a LNAPL-impacted screened casing (equivalent to a LNAPL-impacted observation well) based on the capillary pressure model of Brooks and Corey (1964). In the present study, for purposes of simplification, fluid heights were used instead of capillary pressures. However, capillary pressures are also consistent for determining the displacement heights of different systems (air/LNAPL, LNAPL/water and air/water systems).

3.1 Predicting free LNAPL in soil (h_N)

Field methods exist for evaluating the actual LNAPL thickness in soil based on the Bail-Down test conducted in an observation well (e.g., Gruszcenski, 1987; Hughes et al., 1988; Yaniga and Demko, 1983). However, this type of test would need to be repeated for each of the 15 measurement events undertaken at the impacted site, because the actual LNAPL thickness in soil would not be constant; it varies under the influence of the water table fluctuations. This test may result in complementary fieldwork on a LNAPL-impacted site because any recoverable LNAPL and pumped groundwater would also need to be managed. Despite the valuable contribution of

the Bail-Down test in providing information on the LNAPL distribution in the subsurface, this field test was not undertaken in the present study for technical and management reasons. Instead, the model proposed by Lefebvre and Boutin (2000) is combined in the present study with the Testa and Winegardner (1991) method—to predict the actual thickness of LNAPL in soil—by integrating water table level and apparent LNAPL thickness measurements which were periodically collected over four months of monitoring. Such an approach results in less fieldwork, less data processing, and no need to manage the pumped free LNAPL. The thickness of free LNAPL in soil (Step 1 in Figure 3) is defined as the interval where LNAPL is present in soil at a pressure that is equal to or greater than the atmospheric pressure. Figure 4 shows that the thickness of LNAPL in soil (h_N) can be obtained by Equation 2, i.e., it is the difference between the apparent LNAPL thickness in the observation well (H_N) and the LNAPL/water displacement height (h_d^{NW}). H_N (Step 3 in Figure 3) was measured during each measurement event, while h_d^{NW} (Step 4 in Figure 3) can be calculated according to Equation 3, in which ρ_W and ρ_N are the density of water (1000 kg/m^3) and the density of LNAPL (690 kg/m^3 that has been measured in laboratory), respectively, where the gravitational acceleration (g) is 9.81 m/s^2. The LNAPL/water displacement pressure (p_d^{NW}) in Equation 3 (Step 5 in Figure 3) can be calculated according to the displacement pressure equation—for capillary tubes—applied to the LNAPL/water (NW) and air/water (AW) systems as expressed in Equation 4.

$$h_N = H_N - h_d^{NW} \tag{2}$$

$$h_d^{NW} = \frac{p_d^{NW}}{(\rho_W - \rho_N)g} \tag{3}$$

$$p_d^{NW} = p_d^{AW} \cdot \frac{\sigma_{NW} \cos\theta_{NW}}{\sigma_{AW} \cos\theta_{AW}} \tag{4}$$

In practice, the contact angles θ in Equation 4 are rarely considered explicitly when converting capillary pressure values obtained from different fluid systems (Charbeneau et al., 1995; Lenhard and Parker, 1990; Parker, 1989). This involves the assumption that the fluid is perfectly wetting, where $\theta = 0°$, for all considered fluid systems. The values of the interfacial tension in Equation 4 considered for the LNAPL/water (σ_{NW}) and air/water (σ_{AW}) systems are 48 mN/m (LNAPL constituted of diesel fuel) and 72 mN/m, respectively. The air/water displacement pressure (p_d^{AW}) in Equation 4 (Step 6 in Figure 3) can be obtained by firstly calculating water/air displacement height (h_d^{AW}), and secondly, converting the calculated h_d^{AW} to p_d^{AW}. The h_d^{AW} can be converted to p_d^{AW} with a conversion factor of 98.1 Pa/cm of water according to the hydrostatic pressure effect (e.g., for h_d^{AW} of 68 cm, the p_d^{AW} would be of 6.68 kPa). In Figure 4, the Lefebvre and Boutin's model shows that the h_d^{AW} (Equation 5) (Step 7 in Figure 3) represents the distance between the top elevation of free LNAPL in the observation well (Z_{AN}) and the initial elevation of water table without effect or pressure from LNAPL (Z_{AW}).

$$h_d^{AW} = Z_{AN} - Z_{AW} \tag{5}$$

Let us now describe how Z_{AN} and Z_{AW} are determined. The elevation Z_{AN} (Step 8 in Figure 3) is determined by using Equation 6 that considers the elevation of the top of the monitored well's PVC (Z_{PVC}; Z_{PVC} = 209.10 m GLF), and the LNAPL depth relative to the elevation of the top of the monitored well's PVC. The data regarding LNAPL depth relative to the top of the PVC ($D_{LNAPL/PVC}$) were collected during the measurement events carried out as part of the four months of monitoring.

$$Z_{AN} = Z_{PVC} - D_{LNAPL/PVC} \tag{6}$$

The elevation Z_{AW} (Step 9 in Figure 3) is determined based on the equation of Testa and Winegardner (1991). This equation (Equation 7) makes it possible to theoretically correct the depth of groundwater in an impacted LNAPL observation well by considering the static water table depth, the apparent LNAPL thickness and the LNAPL density. In Equation 7, CD_{WT} is the corrected depth of the water table, SD_{WT} represents the measured static depth of groundwater, H_N is the apparent LNAPL thickness in the observation well, ρ_N represents the density of LNAPL ($\rho_N = 690$ kg/m^3), and ρ_W is water density ($\rho_W = 1000$ kg/m^3). In this study, the SD_{WT} and H_N were collected during the measurement events carried out as part of the four months of monitoring.

$$CD_{WT} = SD_{WT} - \left(H_N \cdot \frac{\rho_N}{\rho_W} \right) \tag{7}$$

The elevation Z_{AW} is determined by using Equation 8 that includes Z_{PVC} (209.10 m GLF), and the CD_{WT} which is determined according to Equation 7.

$$Z_{AW} = Z_{PVC} - CD_{WT} \tag{8}$$

The elevations Z_{AN} and Z_{AW} together make it possible to calculate h_d^{AW} by using Equation 5 (above). Once h_d^{AW} is calculated, the value is converted to p_d^{AW} using the conversion factor mentioned above, and then used in Equation 4 to calculate the LNAPL/water displacement pressure (p_d^{NW}).

3.2 Predicting displacement height h_d^{AN}

To predict h_d^{AN} (Step 2 in Figure 3), Equation 9 is used, where ρ_N and ρ_A are the densities of LNAPL and of Air, respectively, and g is the gravitational acceleration. The air density—being very low compared to that of LNAPL—has been neglected (Equation 9). The air/LNAPL displacement pressure (p_d^{AN}) in Equation 9 is calculated (Step 10 in Figure 3) by using the displacement pressure equation—for capillary tubes—applied to systems of air/LNAPL (AN) and air/water (AW) (Equation 10). The contact angles θ in Equation 10 were assumed to be equal

to zero. The air/LNAPL (σ_{AN}) and air/water (σ_{AW}) interfacial tensions were considered to be 20 mN/m and 72 mN/m, respectively. These values are combined with p_d^{AW} (already calculated in Step 6 in Figure 3), to calculate p_d^{AN} according to Equation 10, and subsequently be introduced in Equation 9 to obtain h^d_{AN}.

$$H_d^{AN} = \frac{p_d^{AN}}{(\rho_N - \rho_A)\, g} \approx \frac{p_d^{AN}}{\rho_N\, g} \tag{9}$$

$$p_d^{AN} = p_d^{AW} \cdot \frac{\sigma_{AN} \cos\theta_{AN}}{\sigma_{AW} \cos\theta_{AW}} \tag{10}$$

3.3 Elevations corresponding to top and bottom of the total LNAPL thickness

To determine the vertical boundaries of the LNAPL-impacted interval, the elevation of the top ($ZT\ h_{Nt}$) (Step 11 in Figure 3) and bottom ($ZB\ h_{Nt}$) of the total LNAPL thickness in soil (Step 12 in Figure 3) are calculated. In this study, Equations 11 and 12 are used for this purpose, in which Z_{AN} represents the top elevation of free LNAPL in the observation well (as measured during the 4 month of monitoring) (Step 8 in Figure 3). Determination of h_d^{AN} (Step 2 in Figure 3) and h_N (Step 1 in Figure 3) for Equations 11 and 12 were described in the previous sections 3.2 and 3.1, respectively.

$$ZT\ h_{Nt} = Z_{AN} + h_d^{AN} \tag{11}$$

$$ZB\ h_{Nt} = Z_{AN} - h_N \tag{12}$$

4 Results and discussions

The field data collected regarding the LNAPL depth relative to the top of the well's PVC ($D_{LNAPL/PVC}$), and the water table depth, also relative to the top of the well's PVC (SD_{WT}) during the four months of monitoring are presented in Table 1. This table also includes the results—

obtained by following the methodology described in the previous section—for the systems' displacement pressure (p_d^{AW}, p_d^{NW} and p^d_{AN}) and systems' displacement height (h_d^{AW}, h_d^{NW} and h_d^{AN}). These calculations made it possible to predict the total LNAPL thicknesses in the soil (h_{Nt}) and determine the elevations corresponding to the top and bottom of the LNAPL-impacted soil interval. According to Table 1, h_{Nt} ranged from 0.13 m (December 5, 2013) to 0.32 m (February 10, 2014). The water table fluctuations raised the free LNAPL to its highest elevation of 206.63 m GLF (February 10, 2014), while the lowest elevation was 205.70 m GLF (December 11, 2013). Accordingly, the thickness of the impacted soil at the monitored well was 0.93 m (206.63 m GLF - 205.70 m GLF). Using the elevation of the ground surface at 209.12 m GLF, the LNAPL-impacted soil was located at the interval depth ranging from 2.49 m (209.12 m GLF - 206.63 m GLF) to 3.42 m (209.12 m GLF - 205.70 m GLF) below ground surface. It should be noted that the total thickness of LNAPL-impacted soil in the present study is predicted based only on 15 measurement events carried out as part of four months of monitoring. Other water table fluctuations—influencing total thickness of LNAPL-impacted soil—may potentially have occurred but were not recorded. The thickness of 0.93 m relative to the LNAPL-impacted soil is evaluated according to the thickness of free, entrapped, and residual LNAPL present in soil. The presence of residual LNAPL in the soil was attributed to all soil pathways where free LNAPL was present. However, complementary measurements of the soil residual LNAPL saturation are recommended for future similar studies to confirm LNAPL saturation over the soil pathways. Figure 5 shows the evolution of the residual LNAPL in the soil and shows the vertical distribution of the total LNAPL thickness in the soil (h_{Nt}) determined according to the 15 measurement events undertaken during four months of monitoring.

Table 1. Data collected during the measurement events during four months of monitoring and results obtained following data processing.

Date/parameter	Depth LNAPL/ PVC	LNAPL elevation	Water table depth/ PVC	Appar. LNAPL thickn.	Correc. depth of water table	Initial elevation of water table	Displ. height Water-Air	Displ. pressure Water/Air	Displ. pressure LNALP/ Water	Displ. height LNAPL/ Water	Actual LNAPL thick. in soil	Displ. Pressure NALP/Air	Displ. height LNAPL/ Air	Total LNAPL thichn. in soil	Elevation of top of h_{Nt}	Elevation of the bottom of h_{Nt}
Prefix	$D_{LNAPL/PVC}$	Z_{AN}	SD_{WT}	H_N	CD_{WT}	Z_{AW}	h_d^{AW}	p_d^{AW}	p_d^{NW}	h_d^{NW}	h_N	p_d^{AN}	h_d^{AN}	h_{Nt}	ZT_{hNt}	ZB_{hNt}
Unit	(m)	(m GLF)	(m)	(m)	(m)	(m GLF)	(m)	(kPa)	(kPa)	(m)	(m)	(kPa)	(m)	(m)	(m GLF)	(m GLF)
Equ. Nr in the text	-	6	-	-	7	8	5	-	4	3	2	10	9	1	11	12
2013-11-11	2.89	206.21	3.30	0.41	3.02	206.08	0.13	1.25	0.83	0.27	0.14	0.35	0.05	0.19	206.26	206.07
2013-11-27	3.21	205.89	3.58	0.37	3.32	205.77	0.11	1.12	0.75	0.25	0.12	0.31	0.05	0.17	205.94	205.77
2013-11-28	3.24	205.86	3.64	0.40	3.36	205.74	0.12	1.22	0.81	0.27	0.13	0.34	0.05	0.18	205.91	205.73
2013-11-29	3.25	205.85	3.57	0.32	3.35	205.75	0.10	0.97	0.65	0.21	0.11	0.27	0.04	0.15	205.89	205.74
2013-12-02	3.27	205.80	3.59	0.32	3.37	205.73	0.10	0.97	0.65	0.21	0.11	0.27	0.04	0.15	205.87	205.72
2013-12-04	3.15	205.95	3.66	0.51	3.31	205.79	0.16	1.57	1.04	0.34	0.17	0.43	0.06	0.24	206.01	205.78
2013-12-05	3.30	205.80	3.58	0.28	3.39	205.71	0.09	0.85	0.57	0.19	0.09	0.24	0.03	0.13	205.83	205.71
2013-12-06	3.15	205.95	3.64	0.49	3.30	205.80	0.15	1.50	1.00	0.33	0.16	0.42	0.06	0.23	206.01	205.78
2013-12-11	3.31	205.79	3.59	0.28	3.40	205.70	0.09	0.85	0.57	0.19	0.09	0.24	0.03	0.13	205.82	205.70
2014-01-07	2.80	206.30	3.41	0.61	2.99	206.11	0.19	1.85	1.24	0.41	0.20	0.52	0.08	0.28	206.38	206.10
2014-01-08	2.85	206.25	3.45	0.60	3.04	206.06	0.19	1.82	1.22	0.40	0.20	0.51	0.07	0.27	206.32	206.05
2014-01-14	2.80	206.30	3.21	0.41	2.93	206.17	0.13	1.25	0.83	0.27	0.14	0.35	0.05	0.19	206.35	206.16
2014-01-22	2.60	206.50	3.22	0.62	2.80	206.31	0.19	1.88	1.26	0.41	0.21	0.52	0.08	0.28	206.58	206.29
2014-02-10	2.56	206.54	3.25	0.69	2.77	206.32	0.21	2.11	1.41	0.46	0.23	0.59	0.09	0.32	206.63	206.31
2014-02-27	2.59	206.51	3.21	0.62	2.78	206.32	0.19	1.88	1.26	0.41	0.21	0.52	0.08	0.28	206.59	206.30

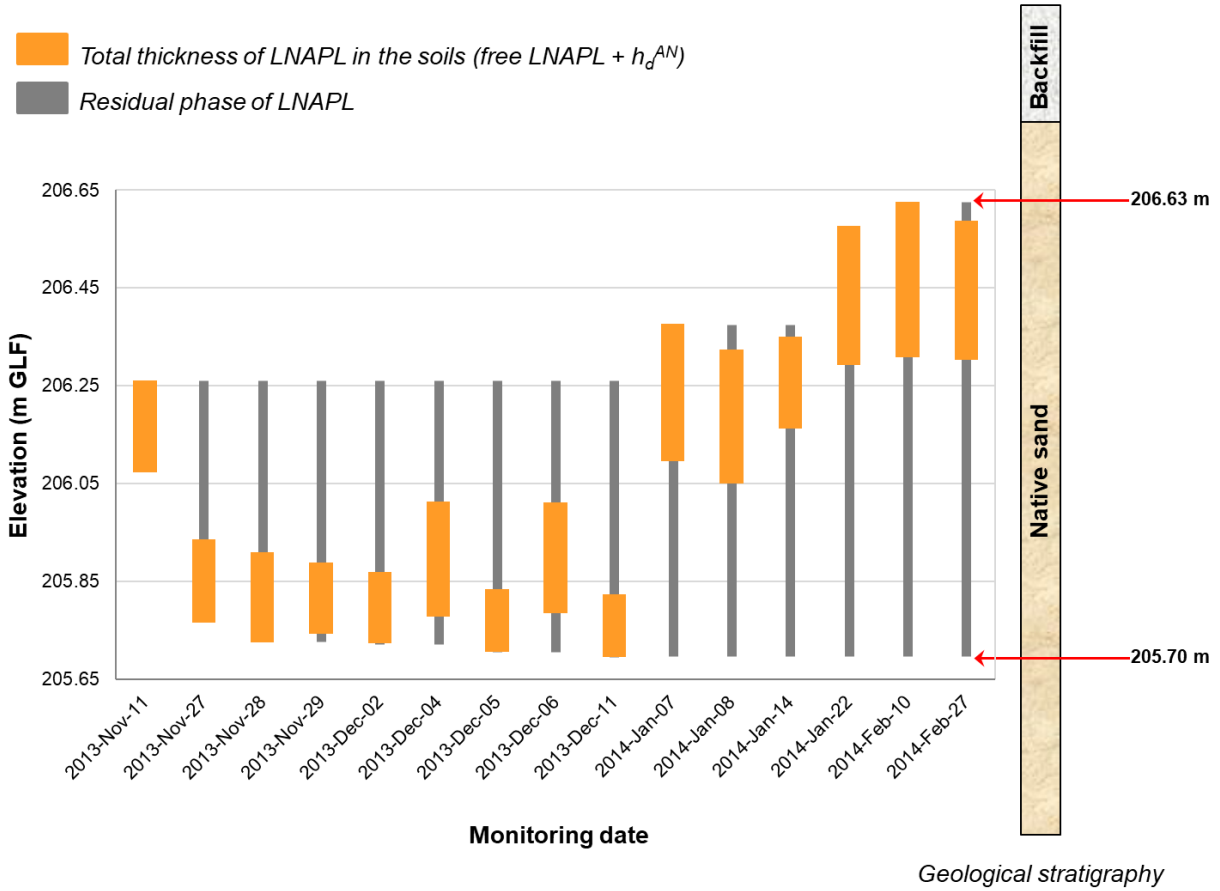

Figure 5. Vertical distribution of LNAPL within the soil relative to water table fluctuations, and gradual evolution of the residual LNAPL phase.

Figure 5 shows the formation of residual LNAPL following the downward displacement of the free LNAPL after November 11, 2013, thus creating a residual LNAPL interval of 32 cm. This thickness was calculated from the difference in elevations between the top of the LNAPL assessed during the first measurement event undertaken on November 11, 2013 (LNAPL top elevation = 206.26 m GLF) and the top of the LNAPL evaluated during the second measurement event conducted on November 27, 2013 (LNAPL top elevation = 205.94 m GLF). During the third measurement event, conducted on November 28, 2013, the LNAPL moved further down and the residual LNAPL thickness increased to 35 cm. This is calculated from the difference in elevations between the top of the LNAPL assessed during the first measurement event, and the top of the LNAPL evaluated from the third measurement event (LNAPL to elevation = 205.91

m GLF). The approach followed in this study made it possible to establish the evolution of the subsurface residual LNAPL interval. Figure 5 shows that the thickness of free LNAPL does not diminish while the residual LNAPL phase increases. This observation may be linked to the LNAPL exchange process, known to cause a delayed interaction relative to water table fluctuations, between LNAPL in the observation well and LNAPL in the soil. Figure 5 shows that the LNAPL movement is entirely contained in the native sand unit of the aquifer. It also shows that following the vertical movement of LNAPL in the subsurface, the soil impacted by residual LNAPL can be located in the aquifer's unsaturated zone, as was the case on December 5, 2013. In this situation, once the free LNAPL has been recovered, an in-situ vadose zone remedial treatment could easily be applied, because the residual LNAPL-impacted interval is not submerged in groundwater. On the other hand, the LNAPL-impacted soil can also be found in the saturated zone, as observed to be the case on February 10, 2014 (Figure 5). In such situations, the methodology proposed in the present study makes it possible to determine how depth the water table should be lowered, by means of pumping, in order that the LNAPL-impacted soil interval may be isolated within an unsaturated zone, so that it can then be subjected to an in-situ vadose zone remedial treatment. Figure 6 shows the variation of the water table depth (SD_{WT} in Table 1) and the predicted free LNAPL-impacted soil thickness (h_{Nt} in Table 1) relative to the measurement event dates. Between the measurement events 1–2, 9–10, and 10–11, it was observed that the water table depth increases while the predicted free LNAPL-impacted soil thickness decreases. As an example, from the measurement event 1 to the subsequent measurement event 2, the water table depth increases from 3.3 to 3.58 m GLF while the predicted free LNAPL-impacted soil thickness decreases from 0.19 to 0.17 m, denoting an inverse correlation between the water table depth and the predicted free LNAPL-impacted soil thickness. However, the predominant relationship observed between the water table depth and the predicted

free LNAPL-impacted soil thickness (across 11 observations out of 14) shows a positive correlation. This means that when the water table level decreases (i.e., water table rises relative to ground surface), the predicted free LNAPL-impacted soil thickness also decreases, and vice versa. Considering the predominant observations, it is suggested that during the highest water table events, a limited soil interval would be vertically impacted by the free LNAPL. However, when enough LNAPL are present, the total LNAPL-impacted soil interval would be encroaching even into the aquifer's saturated zone. Therefore, the observed decreasing free LNAPL-impacted soil thickness, relatively to low water table level occurrences, do not signify less LNAPL-impacted soil interval. But in such a situation, Van De Ven et al. (2021) found that the dynamic effects of water table fluctuations and redistribution of LNAPL into the subsurface affect the short and long-term LNAPL degradation rates. Based on results reported in Table 1, the apparent LNAPL thickness in the observation well (H_N in Table 1) is 3 times greater than the actual free LNAPL thickness in soil (h_N in Table 1) for all the measurement events of the field monitoring. This agrees with investigations stating that the LNAPL thickness measured in a monitoring well has been reported to typically exceed the LNAPL-saturated formation thickness by a factor estimated to range from 2 to 10 (Deska and Ociepa, 2013; Kramer, 1982; Mercer and Cohen, 1990; Yaniga and Demko, 1983). In this study, a factor of 3 is observed to be constant for all the measurement events of the field monitoring, possibly because the LNAPL-impacted soil was located within a single native sand unit of the aquifer. It should be noted that potentially, if this factor were to vary within a single site, this might indicate the presence of heterogeneous stratigraphy. Such a situation might merit further research efforts.

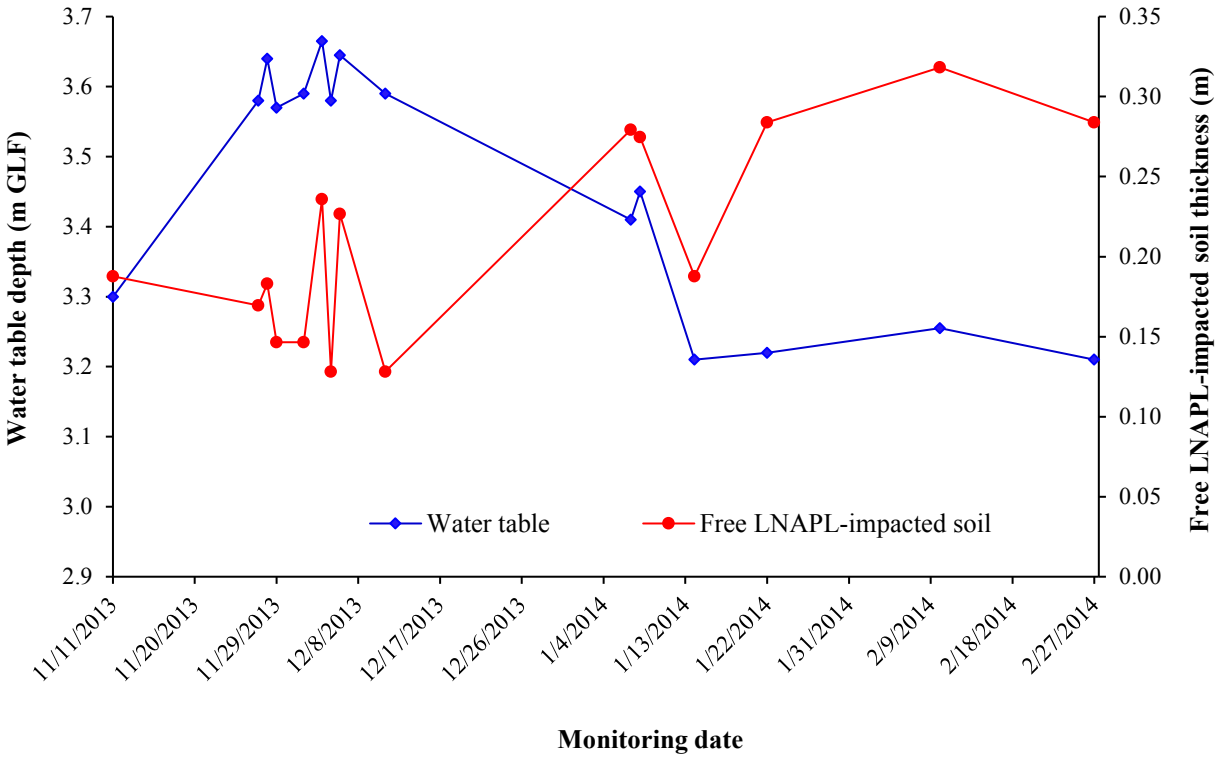

Figure 6. Graphic relationship between water table depth and predicted free LNAPL-impacted soil thickness. The graphic data are from Table 1 (SD_{WT} and h_{Nt}).

5 Summary and conclusions

A methodology is proposed for predicting the vertical distribution of LNAPL-impacted soil in the subsurface by considering the transient effect of water table fluctuations. This proposed methodology relied on water table level and apparent LNAPL thickness measurements, which were periodically collected over four months at a LNAPL-impacted observation well. The vertical LNAPL-impacted soil distribution was predicted by combining information of air/LNAPL and LNAPL/water interface elevations—which were mathematically deduced from Lefebvre and Boutin's model—with the initial elevation of the water table unaffected by LNAPL presence, which is determined by using the Testa and Winegardner method. In this study, all forms of LNAPL—free, entrapped, and residual—were considered as sources of soil contamination and included in the predicted vertical LNAPL-impacted soil distribution. The

present study highlights the capability of the proposed methodology to predict the actual LNAPL-impacted soil thickness in the subsurface without requiring laborious field tests. Our results showed that water table fluctuations raised the free LNAPL in the subsurface to an elevation of 206.63 m GLF, while the lowest elevation was 205.70 m GLF, forming a thickness of 0.93 m of LNAPL-impacted soil. This LNAPL-impacted soil was located only in the native sand unit of the aquifer, and thus did not provide an opportunity to compare the LNAPL behavior in the native sand against its potential behavior in the overlying heterogeneous backfill. Our study finds that the apparent LNAPL thickness is 3 times greater than the actual free LNAPL thickness in soil, and this agrees with previous investigations stating that the apparent LNAPL thickness typically exceeds the LNAPL-saturated formation thickness by a factor ranging from 2 to 10. A positive correlation was generally observed between the water table depth and the predicted free LNAPL-impacted soil thickness, suggesting that the free LNAPL-impacted interval shortens vertically during the highest water table events. Nonetheless, free and residual LNAPL-impacted soil can be located both in the unsaturated and saturated zones of an aquifer. In such situations, the proposed methodology makes it possible to determine how depth the water table should be lowered by means of pumping so that the LNAPL-impacted soil may be isolated only in the unsaturated zone so that it can then be subjected to an in-situ vadose zone treatment. The present study did not aim to estimate the LNAPL saturation and volume of recoverable LNAPL within an aquifer; it focused, rather, on providing an optimum in-situ remediation plan when free LNAPL might be recovered. Practitioners may use the proposed methodology, which is easy to implement, to assess the vertical LNAPL distribution more accurately in a subsurface that is subject to water table fluctuations, and subsequently implement an effective LNAPL remedial program. For future applications, intensive monitoring of water table and free LNAPL fluctuations is recommended to capture the maximum fluctuation events affecting the

distribution of LNAPL-impacted soils. Such monitoring could contribute to reducing uncertainties regarding the determined LNAPL-impacted soil thickness. It was assumed in the present study that the fluids were perfectly wetting; thus, contact angles for different fluid systems were not considered ($\theta = 0°$). For future applications under different conditions (e.g., fluid is not wetting), it is recommended to determine and consider contact angles.

Acknowledgments

The authors thank the Natural Sciences and Engineering Research Council of Canada for funding this project (Grant Nr. RGPIN-2020-04721). The authors also would like to thank the German Research Foundation for supporting this work by funding - EXC2075 – 390740016 under Germany's Excellence Strategy held to Prof. Seyed Majid Hassanizadeh. The authors also acknowledge the support by the Stuttgart Center for Simulation Science (SimTech). The authors thank the environmental consulting company *Sanexen services environnementaux inc*. (Brossard Office in Quebec, Canada) that provided the data for this case study with particular thanks to Ms. Anne-Marie Vaillancourt, Environment team leader and Contaminated sites expert. The authors also thank the owner of the studied site that authorized publication of data for this case study, with the request that its identification be kept confidential. The authors would like to thank Ms. Michelle J. Fraser, National hydrogeology technical leader from Stantec Consulting Limited (Waterloo Office in Ontario, Canada), for her helpful comments and suggestions on improving this manuscript. Professor René Lefebvre from INRS-ETE Quebec (Canada) is thanked for his valuable explanations. Ms. Josée Kaufmann is thanked for editorial collaboration.

References

Adegboye, M.A., Fung, W.K., Karnik, A., 2019. Recent advances in pipeline monitoring and oil leakage detection technologies: Principles and approaches. Sensors (Switzerland) 19, 1–36.

Ahmed, W., Palmier, C., Atteia, O., Class, H., 2019. Multiphase Simulation Model for Validating the Estimate of Light Non-Aqueous Phase Liquids (LNAPL) Transmissivity Using Bail-

Down Test. Arabian Journal for Science and Engineering 44, 6099–6107.
Aral, M., Liao, B., 2002. Effect of groundwater table fluctuations on LNAPL thickness in monitoring wells. Environmental Geology 42, 151–161.
Atteia, O., Palmier, C., Schäfer, G., 2019. On the influence of groundwater table fluctuations on oil thickness in a well related to an LNAPL contaminated aquifer. Journal of Contaminant Hydrology 223, 1–10.
Azimi, R., Vaezihir, A., Lenhard, R.J., Hassanizadeh, M.S., 2020. Evaluation of LNAPL behavior in water table inter-fluctuate zone under groundwater drawdown condition. Water (Switzerland) 12, 1–15.
Ballestero, T.P., Fiedler, F.R., Kinner, N.E., 1994. An Investigation of the Relationship Between Actual and Apparent Gasoline Thickness in a Uniform Sand Aquifer. Groundwater 32, 708–718.
Batu, V., 2012. An Assessment of the Huntley (2000) Baildown Tests Data Analysis Method. Ground Water 50, 500–503.
Brooks, R., Corey, A., 1964. Hydraulic properties of porous media. Hydrology Papers, Colorado State University, Fort Collins 3, 37 pp.
Charbeneau, R.J., 2007. LNAPL Distribution and Recovery Model (LDRM), Volume 1: Distribution and Recovery of Petroleum Hydrocarbon Liquids in Porous Media, API Publication. No. 4760. Washington, DC: American Petroleum Institute.
Charbeneau, R.J., Johns, R.T., Lake, L.W., McAdams, M.J., 2000. Free-product recovery of petroleum hydrocarbon liquids. Ground Water Monitoring and Remediation 20, 147–158.
Charbeneau, R.J., Russel, T.J., Lake, L.W., McAdams, M.J., 1999. Free-product recovery of hydrocarbon liquids, in: American Petroleum Institute, API Pub. 4682, Washington, D.C.
Charbeneau, R.J., Weaver, J.W., Lien, B.K., 1995. The Hydrocarbon Spill Screening Model (HSSM) Volume 2: Theoretical Background and Source Codes. USEPA Publication EPA/600/R-, 1–319.
Chompusri, S., Rivett, M.O., Mackay, R., 2002. LNAPL redistribution on a fluctuating water table: Column experiments. In: Thornton, S.F., Oswald, S.E. (Eds.), Groundwater Quality: Natural and Enhanced Restoration of Groundwater Pollution. IAHS Press, Oxfordshire.
Deska, I., Ociepa, E., 2013. Impact of the water table fluctuations on the apparent thickness of light non aqueous phase liquids. Ecological Chemistry and Engineering A 20, 771–778.
Dippenaar, M.A., Sole, M.D., Van Rooy, J.L., du Toit, G.J., Reynecke, J.L., 2005. Determining actual LNAPL plume thickness: Review and case study in a fractured aquifer. Bulletin of Engineering Geology and the Environment 64, 347–360.
Dokou, Z., Karatzas, G.P., 2013. Multi-objective optimization for free phase LNAPL recovery using evolutionary computation algorithms. Hydrological Sciences Journal 58, 671–685.
Ebrahimi, F., Lenhard, R.J., Nakhaei, M., Nassery, H.R., 2019. An approach to optimize the location of LNAPL recovery wells using the concept of a LNAPL specific yield. Environmental Science and Pollution Research 26, 28714–28724.
EPA, (Environmental Protection Agency), 1996. How to effectively recover free product at leaking underground storage tank sites – Aguide for state regulators. EPA 510-R-96-001.
Farr, A.M., Houghtalen, R.J., McWhorter, D.B., 1990. Volume Estimation of Light Nonaqueous Phase Liquids in Porous Media. Groundwater 28, 48–56.
Frollini, E., Petitta, M., 2018. Free LNAPL volume estimation by pancake model and vertical equilibrium model: Comparison of results, limitations, and critical points. Geofluids 8234167, 1–13.
Gatsios, E., García-Rincón, J., Rayner, J.L., McLaughlan, R.G., Davis, G.B., 2018. LNAPL

transmissivity as a remediation metric in complex sites under water table fluctuations. Journal of Environmental Management 215, 40–48.

Gruszcenski, T.S., 1987. Determination of a realistic estimate of the actual formation product thickness using monitor wells: A field bailout test, in: In National Ground Water Association 1992. Techniques for Estimating the Thickness of Petroleum Products in the Subsurface. NGWA, Anthology, Columbus Ohio.

Hughes, J.P., Sullivan, C.R., Zinner, R.E., 1988. Two techniques for determining the true hydrocarbon thickness in an unconfined sand aquifer., in: National Ground Water Association. 1992. Techniques for Estimating the Thickness of Petroleum Products in the Subsurface. NGWA, Anthology, Columbus Ohio.

Jeong, J., Charbeneau, R.J., 2014. An analytical model for predicting LNAPL distribution and recovery from multi-layered soils. Journal of Contaminant Hydrology 156, 52–61.

Khan, F.I., Husain, T., Hejazi, R., 2004. An overview and analysis of site remediation technologies. Journal of Environmental Management 71, 95–122.

Kramer, W.H., 1982. Ground water pollution from gasoline. Groundwater Monitoring and Remediation 2, 18–22.

Lefebvre, R., 2010. Écoulement multiphase en milieu poreux. Institut National de la Recherche Scientifique, Québec, Canada.

Lefebvre, R., Boutin, A., 2000. Evaluation of free LNAPL volume and producibility in soils, in: 1st Joint IAH-CNC and CGS Groundwater Specialty Conference, 53rd Canadian Geotechnical Conference, Montréal, Canada. pp. 143–150.

Lekmine, G., Sookhak Lari, K., Johnston, C.D., Bastow, T.P., Rayner, J.L., Davis, G.B., 2017. Evaluating the reliability of equilibrium dissolution assumption from residual gasoline in contact with water saturated sands. Journal of Contaminant Hydrology 196, 30–42.

Lenhard, R.J., Johnson, T.G., Parker, J.C., 1993. Experimental observations of nonaqueous-phase liquid subsurface movement. Journal of Contaminant Hydrology 12, 79–101.

Lenhard, R.J., Parker, J.C., 1990. Estimation of Free Hydrocarbon Volume from Fluid Levels in Monitoring Wells. Groundwater 28, 57–67.

Lenhard, R.J., Raynera, J.L., Davisa, G.B., 2017. A practical tool for estimating subsurface LNAPL distributions and transmissivity using current and historical fluid levels in groundwater wells: Effects of entrapped and residual LNAPL. Journal of Contaminant Hydrology 205, 1–11.

Lenhard, R.J., Sookhak Lari, K., Rayner, J.L., Davis, G.B., 2018. Evaluating an Analytical Model to Predict Subsurface LNAPL Distributions and Transmissivity from Current and Historic Fluid Levels in Groundwater Wells: Comparing Results to Numerical Simulations. Groundwater Monitoring and Remediation 38, 75–84.

Marinelli, F., Durnford, D.S., 1996. LNAPL thickness in monitoring wells considering hysteresis and entrapment. Ground Water 34, 405–414.

Matos de Souza, M., Oostrom, M., White, M.D., Da Silva Jr, G.C., Barbosa, M.C., 2016. Simulation of subsurface multiphase contaminant extraction using a bioslurping well model. Transport in Porous Media 114, 649–673.

Mercer, J.W., Cohen, R.M., 1990. A review of immiscible fluids in the subsurface: Properties, models, characterization and remediation. Journal of Contaminant Hydrology 6, 107–163.

Millette, D., Gosselin, C., Béliveau, É., 2014. Clean-up at Lac-Mégantic : the tragic oil spill and explosion in a Québec town left a trail of contamination in its wake : consulting engineers were immediately called in to help contain the damage. Canadian consulting engineer 55, 12–16.

Mobile, M., Widdowson, M., Stewart, L., Nyman, J., Deeb, R., Kavanaugh, M., Mercer, J., Gallagher, D., 2016. In-situ determination of field-scale NAPL mass transfer coefficients: Performance, simulation and analysis. Journal of Contaminant Hydrology 187, 31–46.

Palmier, C., Cazals, F., Atteia, O., 2017. Bail-Down Test Simulation at Laboratory Scale. Transport in Porous Media 116, 567–583.

Parker, J.C., 1989. Multiphase flow and transport in porous media. Reviews of Geophysics. https://doi.org/10.1029/RG027i003p00311

Parker, J.C., Kim, E., Widdowson, M., Kitanidis, P., Gentry, P., 2010. Effects of model formulation and calibration data on uncertainty in predictions of DNAPL source dissolution rate. Water Resource Research 46, 1–11.

Parker, J.C., Zhu, J.L., Johnson, T.G., Kremesec, V.J., Hockman, E.L., 1994. Modeling Free Product Migration and Recovery at Hydrocarbon Spill Sites. Groundwater 32, 119–128.

Pasha, A.Y., Hu, L., Meegoda, J.N., 2014. Numerical simulations of a light nonaqueous phase liquid (LNAPL) movement in variably saturated soils with capillary hysteresis. Canadian Geotechnical Journal 51, 1046–1062.

Qin, X., Huang, G., Yu, H., 2009. Enhancing remediation of LNAPL recovery through a response-surface-based optimization approach. Journal of Environmental Engineering 135, 999–1008.

Sookhak Lari, K., Davis, G.B., Rayner, J.L., Bastow, T.P., Puzon, G.J., 2019. Natural source zone depletion of LNAPL: A critical review supporting modelling approaches. Water Research 157, 630–646.

Sookhak Lari, K., Rayner, J.L., Davis, G.B., 2018. Towards characterizing LNAPL remediation endpoints. Journal of Environmental Management 224, 97–105.

Sookhak Lari, K., Rayner, J.L., Davis, G.B., Johnston, C.D., 2020. LNAPL Recovery Endpoints: Lessons Learnt Through Modeling, Experiments, and Field Trials. Groundwater Monitoring and Remediation 40, 21–29.

Steffy, D.A., Johnston, C.D., Barry, D.A., 1998. Numerical simulations and long-column tests of LNAPL displacement and trapping by a fluctuating water table. Soil and Sediment Contamination 7, 325–356.

Steffy, D.A., Johnston, C.D., Barry, D.A., 1995. A field study of the vertical immiscible displacement of LNAPL associated with a fluctuating water table. In: Kovar, K., Kr_asný, J. (Eds.), Groundwater Quality: Remediation and Protection. IAHS Press, Oxfordshire.

Suthersan, S.S., Horst, J., Schnobrich, M., Welty, N., McDonough, J., 2017. Remediation Engineering: Design Concepts. Second ed. CRC Press Taylor & Francis Group, Boca Raton, FL, USA.

Testa, S.M., Winegardner, D.L., 1991. Restoration of Petroleum Contaminated Aquifers: Petroleum Hydrocarbons and Organic Compounds. Second Edition, CRC Press Taylor & Francis Group, Boca Raton London New York.

Tomlinson, D.W., Rivett, M.O., Wealthall, G.P., Sweeney, R.E., 2017. Understanding complex LNAPL sites: illustrated handbook of LNAPL transport and fate in the subsurface. Journal of Environmental Management 204, 748–756.

Van Dam, J., 1967. The migration of hydrocarbons in a water-bearing stratum, in: The Joint Problems of the Oil and Water Industries. Institute of Petroleum, London, UK, pp. 55–96.

Van De Ven, C.J.C., Scully, K.H., Frame, M.A., Sihota, N.J., Mayer, K.U., 2021. Impacts of water table fluctuations on actual and perceived natural source zone depletion rates. Journal of Contaminant Hydrology 238, 1–13.

Wagner, R.B., Hampton, D.R., Howell, J.A., 1989. A new tool to determine the actual thickness

of free product in a shallow aquifer, in: Proceedings of the Conference on Petroleum Hydrocarbons and Organic Chemicals in Ground Water : Prevention, Detection and Restoration, Houston, Texas. pp. 45–59.

White, M.D., Oostrom, M., Lenhard, R.J., 2004. A practical model for mobile, residual, and entrapped NAPL in water-wet porous media. Ground Water 42, 734–746.

Yaniga, P.M., Demko, D.J., 1983. Hydrocarbon contamination of carbonate aquifers: Assessmet and abatement, in: Proceedings of the Third National Symposium on Aquifer Restoration and Ground-Water Monitoring, Columbus, Ohio. National Water Well Association, pp. 60–65.